RTDF2007-46010

ANALYSES OF FULL-SCALE TANK CAR SHELL IMPACT TESTS

Y.H. Tang
Volpe National Transportation Systems Center
Cambridge, Massachusetts, USA

H. Yu
Chenga Advanced Solutions & Engineering, LLC
Cambridge, Massachusetts, USA

J.E. Gordon
Volpe National Transportation Systems Center
Cambridge, Massachusetts, USA

M. Priante
Volpe National Transportation Systems Center
Cambridge, Massachusetts, USA

D.Y. Jeong
Volpe National Transportation Systems Center
Cambridge, Massachusetts, USA

D.C. Tyrell
Volpe National Transportation Systems Center
Cambridge, Massachusetts, USA

A.B. Perlman
Volpe National Transportation Systems Center
Cambridge, Massachusetts, USA

ABSTRACT

This paper describes analyses of a railroad tank car impacted at its side by a ram car with a rigid punch. This generalized collision, referred to as a shell impact, is examined using nonlinear finite element analysis (FEA) and three-dimensional (3-D) collision dynamics modeling. Moreover, the analysis results are compared to full-scale test data to validate the models. Commercial software packages are used to carry out the nonlinear FEA (ABAQUS and LS-DYNA) and the 3-D collision dynamics analysis (ADAMS). Model results from the two finite element codes are compared to verify the analysis methodology. Results from static, nonlinear FEA are compared to closed-form solutions based on rigid-plastic collapse for additional verification of the analysis. Results from dynamic, nonlinear FEA are compared to data obtained from full-scale tests to validate the analysis. The collision dynamics model is calibrated using test data. While the nonlinear FEA requires high computational times, the collision dynamics model calculates gross behavior of the colliding cars in times that are several orders of magnitude less than the FEA models.

INTRODUCTION

Comprehensive data on tank car accident damage have been collected since the late 1960s by the Railroad Tank Car Safety Research and Test Project, which is co-sponsored by the Railway Supply Institute and the Association of American Railroads. An evaluation of the data indicates that releases of toxic inhalation hazard (TIH) materials from accident events (e.g., collisions and derailments) are commonly caused by failures in three general locations: (1) tank car head or end cap, (2) tank car shell or side, and (3) fittings [1]. Two recent accidents that led to the release of hazardous materials (hazmat) occurred from impacts and penetrations to the head [2] and the shell [3]. Moreover, the structural integrity of railroad tank cars involved in accidents was brought to the forefront of research after the National Transportation Safety Board (NTSB) published its findings of the train derailment that occurred in Minot, North Dakota on January 18, 2002 [4]. As a result of its Minot accident investigation, NTSB made several safety recommendations to the Federal Railroad Administration (FRA) concerning railroad tank cars. In its role to provide technical support to FRA, the Volpe National Transportation Systems Center (Volpe Center) developed a research program to address NTSB concerns. This research program began in 2004, and entails the development of computational tools and validation through testing.

In 2006, Dow Chemical Company, Union Pacific Railroad, and Union Tank Car Company began an industry research and development effort called the Next-Generation Rail Tank Car (NGRTC) Project to develop improved designs for railroad

tank cars carrying hazmat. Since early in 2007, FRA, Transport Canada, and the Volpe Center have been collaborating with the industry sponsors of the NGRTC project to share research information.

This paper describes work that is a product of research conducted to address the NTSB tank car safety recommendations from the Minot accident and work related to the NGRTC Project. The research described in this paper will also be used to support rulemaking for transporting hazmat by railroad tank cars.

Previous research on the vulnerability of tank cars to puncture from impacting objects (such as couplers and wheels from adjacent cars, etc.) has focused on head impacts [5-8]. However, no previous work has been performed to examine shell impacts.

This paper describes nonlinear (i.e., elastic-plastic) finite element models to examine the force-indentation behavior of tank cars from shell impacts. The models are developed using the commercial finite element codes ABAQUS and LS-DYNA. The finite element models are verified by comparing results from both solvers with each other and with known solutions for static loading. The models are then validated with data obtained from full-scale tests that were performed at the Transportation Technology Center in Pueblo, Colorado.

Finite element analysis (FEA) can be used to calculate deformations, stresses, and strains in specific locations within the tank structure. Gross behavior of impacting cars can be readily calculated using collision dynamics models. A three-dimensional collision dynamics model was developed using the force-indentation characteristics from the validated finite element models. Moreover, the collision dynamics model was developed using a commercial software program for rigid multi-body dynamics called Automatic Dynamic Analysis of Mechanical Systems (ADAMS). Results from the collision dynamics model are presented and compared to the full-scale test data.

The collision dynamics model was used to guide the development of the test design and to ensure that the test can be conducted safely and effectively. The model can be used to extrapolate test results for different impact speeds.

FINITE ELEMENT MODEL

Finite element models are developed to examine the deformation and failure of the tank due to impact. The computational times for these models are extensive because the models must include (1) structural dynamics, (2) nonlinear (i.e., elastic-plastic) material behavior, (3) fluid-structure interaction, and (4) material failure.

FEA is readily suitable for analysis of structural dynamics in terms of how a structure moves with time under prescribed loads.

Elastic-plastic material behavior is modeled using a Ramberg-Osgood equation for strain as a function of stress,

$$\varepsilon = \frac{\sigma}{E} + \left(\frac{\sigma}{K}\right)^n \tag{1}$$

where ε is the strain, σ is the stress, and E is the modulus of elasticity. In addition, n and K are material constants. Table 1 lists the values for these constants assumed for TC-128B tank car steel in the finite element analyses. These constants were derived from the yield and ultimate tensile strengths listed in the table, which correspond to the minimum requirements for this particular tank car steel.

Table 1. Constants and Mechanical Properties Corresponding to Minimum Requirements for TC-128B Tank Car Steel

Constant or property	Value
Modulus of elasticity, E (ksi)	30,000
Hardening exponent, n	9.41
R-O Constant, K (ksi)	96.8
Yield strength (ksi)	50
Tensile strength (ksi)	81

When the tank contains lading, the fluid and the tank structure both move and exert forces upon one another during the impact event. Different mesh representations are used in the finite element models to account for fluid-structure interaction. Specifically, Lagrangian and Eulerian mesh formulations are used. In a Lagrangian mesh, the nodes follow the material as it deforms. An Eulerian mesh is fixed in space, and tracks the material passing through. A Lagrangian mesh is used to model the tank structure. Both Lagrangian and Eulerian mesh formulations are used to model the fluid.

Prediction of material failure in a crack-free structure requires application of a reliable fracture initiation criterion. An evaluation of several criteria was recently conducted to examine their merits [9]. In the present work, a criterion based on stress triaxiality [10] was used to predict failure by puncture in the full-scale impact tests. Briefly, stress triaxiality describes the portion of the stress tensor that is hydrostatic. The failure criterion based on stress triaxiality was calibrated using data from pendulum impact tests conducted on un-notched Charpy specimens made from TC-128 tank car steel [11]. The analysis on the unnotched Charpy tests provides a benchmark for which the failure criterion can be applied to the full-scale tests.

Credibility is built into the models by conducting various activities referred to as Verification and Validation (V&V). Verification assesses the accuracy of the solutions from the computational models by comparing model results with known solutions. Validation assesses the accuracy of the computational simulation by comparing model results with data. Moreover, verification means that the mathematics associated with the

model are being calculated correctly, and validation means that the physics are being modeled properly.

Verification

Closed-form solutions are available in the open literature for large plastic deformations of cylindrical tubes subjected to various static loading conditions, including lateral loads [12-13]. The closed-form solutions assume rigid-plastic material behavior, which confines the deformation within a narrow region. Moreover, the deformation behaves as a mechanism or a system of rigid bars linked by hinges such that the motion of the system takes place through rotations at the hinges. In addition, the closed-form solutions are strongly sensitive to the assumed boundary conditions.

Figure 1 compares the closed-form force-indentation curve for the plastic deformation of a cylindrical tube under lateral loading to that from a static, elastic-plastic FEA using ABAQUS. The cylinder is assumed to rest on a rigid surface on the opposite side from the applied lateral load, and is free to slide and rotate at its ends. Moreover, the comparison between the FEA result and the closed-form solution shows reasonable agreement. The effects of internal pressure and fluid lading are not included.
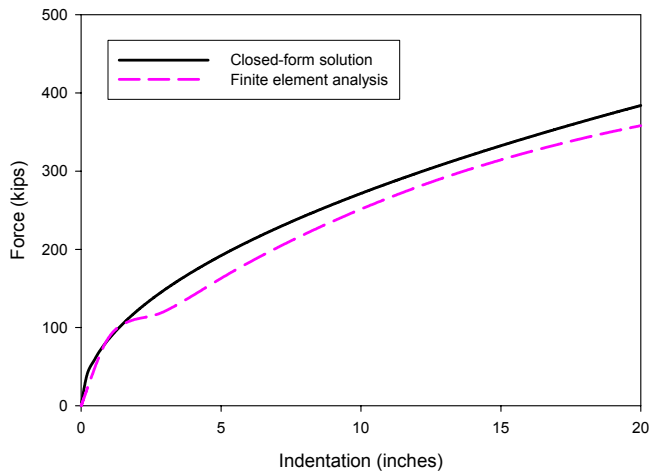
Figure 1. Static Force-Indentation Curves from Closed-Form Solution and FEA

Figure 2 compares static results from ABAQUS with dynamic results at two different impact speeds (16 and 20 mph) from LS-DYNA. The figure demonstrates that the analyses are producing similar results. Moreover, the comparisons provide further verification of the modeling development.
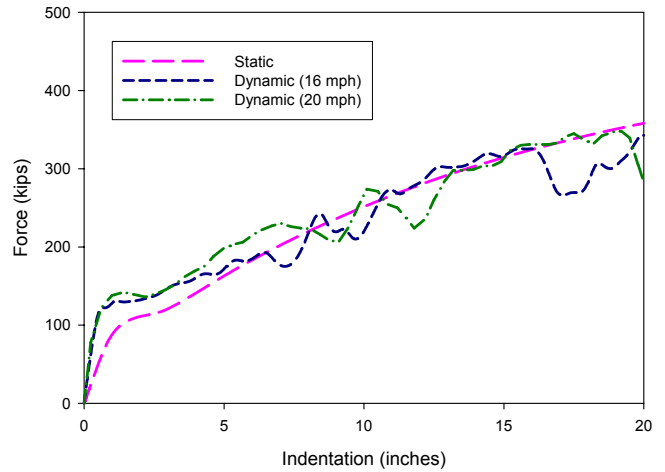
Figure 2. Force-Indentation Curves from Static and Dynamic Elastic-Plastic FEA

Validation

Three full-scale tank car shell impact tests were performed to validate the finite element models. In these tests, the tank car was positioned next to a concrete wall, as shown in Figure 3.

Figure 3. Position of Tank Car in Full-Scale Tests

The tank car contains water mixed with clay slurry to produce the density approximately equal to that of liquid chlorine. The outage in the tests is 10.6 percent with an internal pressure of 100 psi. A ram car weighing 286,000 lb with a rigid impactor was used to strike the side of tank car at its center on the beltline. The couplers at each end of the tank car were removed, and replaced with outriggers to support the tank car as it rebounded off the wall after impact. The

outriggers were L-shaped beams installed in the draft pockets, which were supported by wood blocks. These outriggers were used in the first two tests. A new design, referred to as skids, was used in the third test to reduce the gross motion of the tank car during impact.

Table 2 briefly summarizes the three full-scale shell impact tests in terms of impact speeds and outcomes. The first test, called the Assurance Test (also referred to as Test 0), was conducted to understand the test environment and the gross motions of the cars during the impact test. Moreover, the cars in Test 0 were equipped with limited instrumentation. The cars in subsequent tests were heavily instrumented to provide redundant measurements for forces and displacements. In addition, different impactor sizes were used in the tests, which are denoted in the table. The impactor shape was a rectangular cross-section with rounded edges. Different impactor sizes were used in the full-scale tests. The dimensions for each impactor face are listed in Table 3. Test 2 was originally intended to be run at 14 mph, so that only one variable (impactor size) would be varied. However, a slightly higher impact speed of 15 mph was targeted in Test 2.

Table 2. Full-Scale Tank Car Shell Impact Tests

	Impact Speed (mph)	Impactor	Outcome
Test 0	10	1	Tank integrity maintained, 4-inch residual dent depth
Test 1	14	1	Tank integrity maintained, 9-inch residual dent depth
Test 2	15	2	Tank punctured

Table 3. Dimensions of Impactor Faces

Impactor	Width (inches)	Height (inches)	Edge Radii (inch)
1	17	23	1
2	6	6	½

The finite element models to simulate the full-scale tests do not include tank car components such as the manway, body bolsters, and draft sills. In addition, the presence of the thermal protection is ignored for all tests and the presence of the steel jacket is ignored for both Test 0 and Test 1.

Assurance Test

In all of the tests, the ram car was instrumented with accelerometers. The accelerometer data were filtered, and processed to provide forces. Figure 4 compares the force-time history as measured in Test 0 with those calculated from the finite element models. Results from different fluid formulations to account for fluid-structure interaction are shown in the figure. These results suggest that the Eulerian fluid formulation provides the most accurate results in terms of capturing the overall character of the force-time history. Moreover, these results suggest that the movement or sloshing of the fluid during the impact event plays a significant role in the force-time behavior.
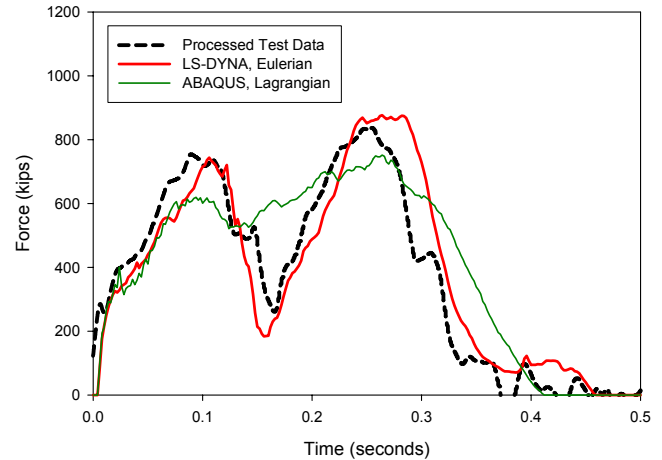
Figure 4. Comparison of Force-Time Histories for Test 0

Table 4 compares the maximum impact force measured in Test 0 with results from the FEA with different fluid formulations. The maximum impact force calculated using LS-DYNA with the Eulerian fluid formulation is within 5 percent of the test data, which is excellent agreement.

Table 4. Comparison between Test 0 and FEA

	Maximum Force (kips)
Assurance Test	837
LS-DYNA, Eulerian	877
ABAQUS, Lagrangian	707

Full-Scale Shell Impact Test 1

The accelerometer measurements in Shell Impact Test 1 were filtered and processed in the same manner as in the Assurance Test. Figure 5 compares the force-time histories from the data and the FEA using LS-DYNA with the Eulerian fluid representation, which again shows excellent agreement.
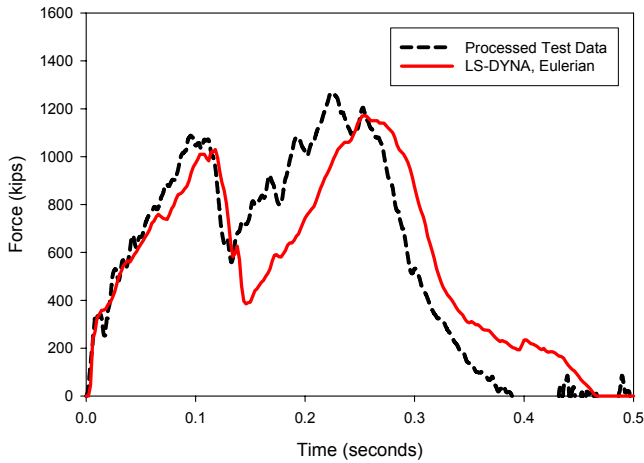
Figure 5. Comparison of Force-Time Histories for Test 1

Figure 6. Overlay of Deformed Shape from FEA Simulation on Still Frame from High-Speed Movie

Table 5 compares the maximum impact forces and maximum indentations from Test 1 and the FEA results using LS-DYNA with the Eulerian fluid formulation. The maximum impact forces are within 10 percent. Figure 6 is a still photograph taken during the test with the FEA simulation overlaid. The figure indicates that the analysis provides a reasonable simulation for the overall deformation of the tank in the test.

The maximum indentation of 26 inches was measured in the test with string potentiometers, compared to the FEA prediction of 30 inches. The FEA prediction was a calculation performed prior to the test assuming the minimum requirements for mechanical properties of TC-128B tank car steel. After Test 1 was conducted, tensile tests were performed to determine the actual mechanical properties, which were roughly 10 percent greater than the minimum requirements for both yield and ultimate tensile strengths. The FEA calculations were conducted with the actual properties, which resulted in slightly better agreement for both maximum impact force and maximum indentation (Table 5).

Table 5. Comparison between Test 1 and FEA

	Maximum Force (kips)	Maximum Dent (inches)
Test 1 Data	1290	26
LS-DYNA, Eulerian [1]	1223	29
LS-DYNA, Eulerian [2]	1170	30

NOTES:
[1] Based on material properties measured from Test 1 tank car
[2] Based on minimum requirements for mechanical properties

A key output from the FEA is the force-indentation characteristic. Figure 7 compares the curves from the test data and the FEA results. The curve from the test data is a cross-plot of indentation-time history from the string potentiometers and force-time history from the processed accelerometer data. The force-indentation curve from the FEA shows qualitative agreement with the test. Both curves show the drop in force due to the movement of the fluid during the impact event. In addition, both curves show nonlinear, dynamic recovery of the indentation. That is, the test data shows that the maximum indentation 26 inches, but the permanent or residual dent depth is about 9 inches. The maximum indentation and residual dent calculated by the FEA assumed the minimum required mechanical properties for TC-128B tank car steel.
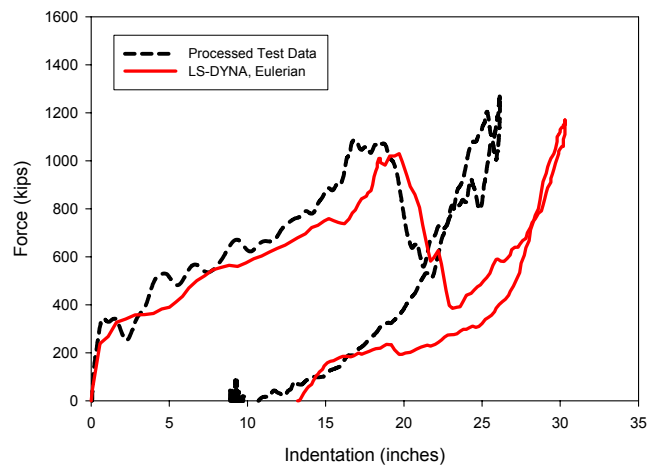
Figure 7. Comparison of Force-Indentation Curves for Test 1

Full-Scale Shell Impact Test 2

The second full-scale shell impact test used an impactor with a smaller cross-sectional area than the previous tests (recall Table 3) to increase the likelihood of rupturing the tank during the test. Moreover, the impacting car in this test struck the side of the tank car at 15 mph, and created a puncture.

Analyses of Test 0 and Test 1 demonstrated that the FEA with the Eulerian fluid formulation provides results that more closely resemble the test data. However, the present capabilities of the software are such that material failure was incorporated into the FEA with the Lagrangian fluid formulation only. Moreover, material failure is assumed to initiate when the effective strain reaches a certain value for a given state of stress in terms of stress triaxiality [11].

The fracture of unnotched Charpy specimens was examined and was shown to provide a benchmark in applying the failure criterion. The failure criterion based on stress triaxiality was then applied to examine the puncture resistance of the tank car in Test 2.

The accelerometer measurements in Shell Impact Test 2 were filtered and processed in the same manner as the previous tests. Figure 8 compares the force-time histories from Test 2 with finite element analyses with and without applying the failure criterion. The figure shows that the processed force data quickly drops off at about 90 milliseconds, indicating the time at which failure of the tank initiated and eventually led to puncture. The data also indicates that the impact force at the time of failure was 910 kips. The force-time history curves from the FEA with and without the failure criterion are nearly identical up to 90 milliseconds. The force drop-off calculated by the FEA with the failure criterion occurs slightly earlier than the test. In addition, the maximum force calculated by the FEA with the failure criterion is lower than the peak impact force measured in Test 2. These differences are attributed to the new skid design for Test 2 in which the tank car is positioned next to the wall. That is, the skid design may provide more structural stiffening to the tank than the previous outrigger design used in the previous tests. The overall character of the calculated force-time history resembles the test data reasonably well.

FEA of Test 2 assumed material properties measured from the tank car used in Test 1, which are roughly about 10 percent greater than the minimum requirements for both yield strength and ultimate tensile strength.
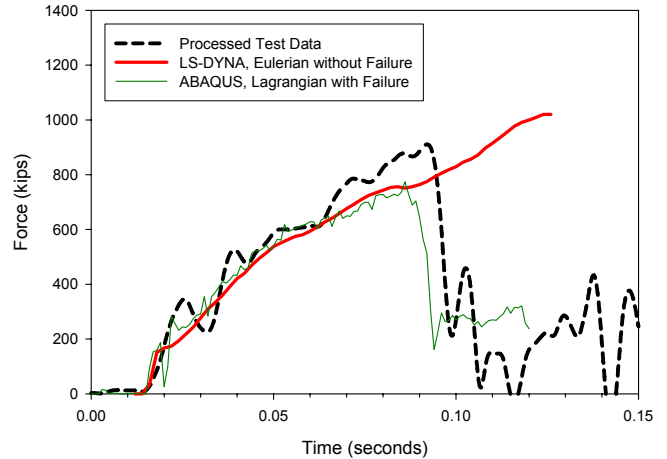
Figure 8. Comparison of Force-Time Histories for Test 2

COLLISION DYNAMICS MODEL

The collision dynamics model consists of a system of springs and lumped masses, and is implemented using ADAMS, a commercial software program. The model is developed to ensure that the test can be conducted safely and effectively. Moreover, the model can be used to extrapolate test results. The key inputs to this model are the ram car weight (286 kips), the tank car weight (241 kips), and the force-displacement characteristics for the tank structure and suspension elements. The outputs from the model are gross motions of the ram and tank cars such as linear and angular displacement, velocity and acceleration (equivalent to force).

Figure 9 shows a schematic of the masses representing the tank car fluid and shell. Not shown are masses and suspension for the trucks on the tank and ram cars. The entire tank is represented by three masses; one for the fluid and two for the tank structure, each representing half of the tank's mass. An elastic spring connects the two masses representing the tank. Elastic springs also connect the fluid to the tank. The value of these spring constants is chosen to represent the frequency of the fluid movement relative to the tank.
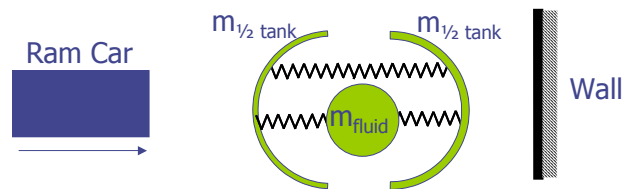
Figure 9. Tank and Fluid Masses Connected by Springs

Figure 10 shows the force-displacement characteristic derived using processed accelerometer data from the ram car in Test 1.
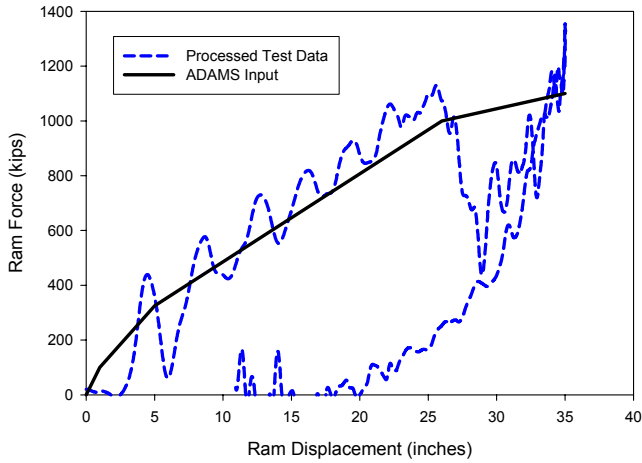
Figure 10. Force-Displacement for Ram Car Impacting Tank

Still photographs from the high-speed cameras of Test 1 are shown in Figure 11. The three stills show the time at which 1) the indenter of the ram car makes contact with the tank car, 2) the maximum penetration the indenter into the tank, 3) and the final dent size when the indenter is no longer contacting the tank car. The roll of the tank car can be observed in these stills. In the first image, the tank car is positioned upright on its trucks. In the second image the tank car is fully supported by the wall and reaches a maximum roll in the clockwise direction of approximately 6 degrees. In the final image, the tank car has returned to its original position.

Similarly Figure 12 shows a sequence of still photographs from Test 2. The three stills correspond to 1) triggering the instrumentation to start recording, 2) initial contact of the ram car with the tank car, and 3) the initiation of the puncture of the tank. Moreover the roll of the tank car in Test 2 was less than that in the previous tests.

Figure 13 compares displacements calculated using the collision dynamics model with data processed from accelerometers on the vehicles in Test 1. The ram car moves approximately 34 inches into the tank car, reaching its peak displacement at 0.25 seconds after initial contact. The tank car CG (center of gravity) moves approximately 7.5 inches towards the wall.

Figure 11. Stills from Test 1

Figure 12. Stills from Test 2
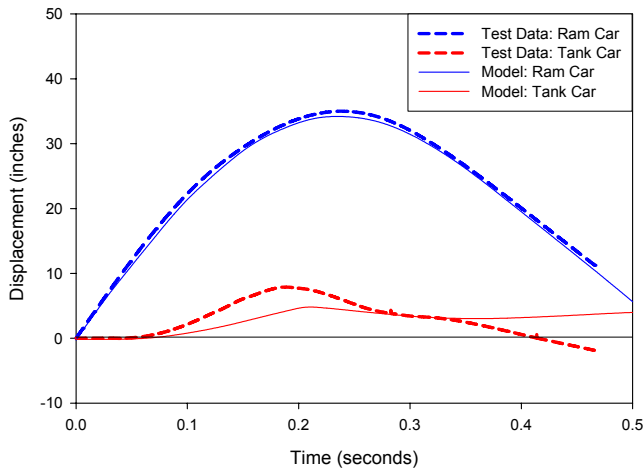
Figure 13. Comparison of Displacement-Time Histories for Test 1

Figure 14 compares the velocity-time histories of the tank car and the ram car for the accelerometer data from Test 1 and the collision dynamics model. The ram car decelerates from 14 mph until it has zero velocity at 0.24 seconds. The model follows the test data quite closely. The tank car velocity increases as it moves towards the wall and then decreases as it rebounds from the wall.
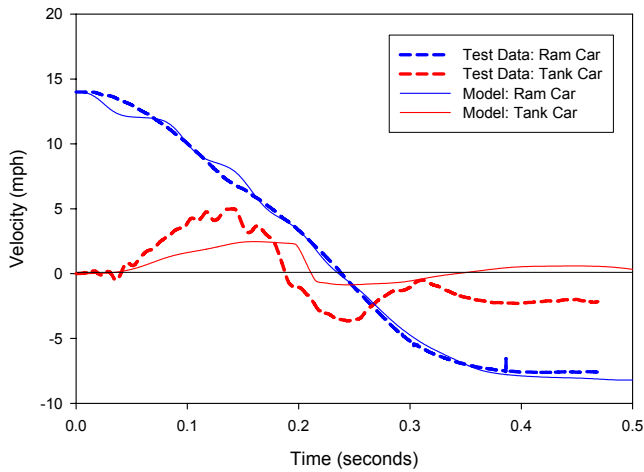
Figure 14. Comparison of Velocity-Time Histories for Test 1

During the conduct of the full-scale tests, the ram car was observed to pitch, and the tank car was observed to roll toward the wall. Figure 15 shows a schematic of these gross motions. The pitching motion occurs because the center of gravity of the

ram car is lower than the point of impact with the tank car. The rolling motion occurs because the structural response of the inner tank, which contains the fluid, does not engage until the combination of thermal insulation materials and steel jacket are crushed against the wall. The layered combination adds roughly 4 inches to the radius of the overall tank, and offers effectively no structural resistance.
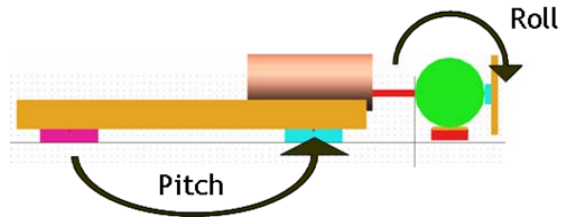
Figure 15. Pitch of Ram Car and Roll of Tank Car

The collision dynamics model was used to calculate the gross motions of the ram and tank cars in the full-scale shell impact tests. Table 6 shows a comparison of the pitch and roll for the first two tests and the model. The tank car roll is calculated using data from accelerometers located on the manway and belly of the tank car.

Table 6. Gross Car Motions in Full-Scale Shell Impact Tests

	Maximum Pitch Ram Car		Maximum Roll Tank Car	
	Test	Model	Test	Model
Test 0	0.25º	0.4º	4.5º	5.7º
Test 1	1º	0.53º	5.75º	5º

The dynamic nonlinear (i.e., elastic-plastic) finite element models with fluid-structure interaction are computationally intensive and require high computational times to execute. The calibrated collision dynamics model requires minimal computational times that are several orders of magnitude less than the FEA models. Moreover, the collision dynamics model can be readily applied to extrapolate results for different impact velocities.

CONCLUDING REMARKS

Elastic-plastic finite element models have been developed to examine the force-indentation behavior of railroad tank cars under shell impact loading conditions. Prior to this work, this type of impact loading condition was not examined. The models were verified by comparing static analysis results to closed-form solutions, which show reasonable agreement. The models were validated by comparing dynamic analysis results

with full-scale impact test data, which showed excellent agreement. Moreover, the verified and validated models can be used to extrapolate structural behavior for different impact scenarios and to develop improved designs to maintain tank integrity under more severe loading conditions than current equipment.

The finite element analyses described in this paper require high computational times due to the complexities in accounting for fluid-structure interaction and material failure as well as dynamic impact loading and nonlinear (i.e., elastic-plastic) material behavior.

Three-dimensional collision dynamics modeling of the full-scale tests has also been conducted. The model results provide reasonable estimates for gross motions of the cars in the full-scale tests. Moreover, the collision dynamics model can be readily applied to extrapolate test results for varying impact speeds.

ACKNOWLEDGMENTS

REFERENCES

[1] Treichel, T., 2006: "List of Accident-Caused Releases of Toxic Inhalation Hazard (TIH) Materials from Tank Cars, 1965-2005," RSI-AAR Railroad Tank Car Safety Research and Test Project, RA 06-05.

[2] National Transportation Safety Board, 2006: "Collision of Union Pacific Railroad Train MHOTU-23 with BNSF Railway Company Train MEAP-TUL-126-D with Subsequent Derailment and Hazardous Materials Release, Macdona, Texas, June 28, 2004," Railroad Accident Report NTSB/RAR-06/03.

[3] National Transportation Safety Board, 2005: "Collision of Norfolk Southern Freight Train 192 With Standing Norfolk Southern Local Train P22 With Subsequent Hazardous Materials Release at Graniteville, South Carolina January 6, 2005," Railroad Accident Report NTSB/RAR-05/04.

[4] National Transportation Safety Board, 2004: "Derailment of Canadian Pacific Railway Freight Train 292-16 and Subsequent Release of Anhydrous Ammonia Near Minot, North Dakota January 18, 2002," Railroad Accident Report NTSB/RAR-04/01.

[5] Phillips, E.A., Olsen, L., 1972: "Final Phase 05 Report on Tank Car Head Study," RPI-AAR Tank Car Safety Research and Test Project, RA-05-17.

[6] Shang, J.C. Everett, J.E., 1972: "Impact Vulnerability of Tank Car Heads," *Shock and Vibration Bulletin 42,* 197-210.

[7] Coltman, M., Hazel, M., 1992: "Chlorine Tank Car Puncture Resistance Evaluation," Volpe National Transportation Systems Center, Report DOT/FRA/ORD-92/11.

[8] Jeong, D.Y., Tang, Y.H., Yu, H., Perlman, A.B., 2006: "Engineering Analyses for Railroad Tank Car Head Puncture," *Proceedings of IMECE2006*, 2006 ASME International Mechanical Engineering Congress and Exposition, IMECE2006-13212.

[9] Wierzbicki, T., Bao, Y.B., Young-Woong, L., Yuanli, B., 2005: "Calibration and evaluation of seven fracture models," *International Journal of Mechanical Sciences 27,* 719-743.

[10] Bao, Y., Wierzbicki, T., 2004: "On fracture locus in the equivalent strain and stress triaxiality space," *International Journal of Mechanical Sciences 46,* 81-98.

[11] Yu, H., Jeong, D.Y., Gordon, J.E., Tang, Y.H., 2007: "Analysis of Impact Energy to Fracture Unnotched Charpy Specimens Made from Railroad Tank Car Steel," *Proceedings of the 2007 ASME Rail Transportation Division Fall Technical Conference,* RDTF2007-46038.

[12] Wierzbicki, T., Suh, M.S., 1988: "Indentation of Tubes under Combined Loading," *International Journal of Mechanical Sciences 30,* 229-248.

[13] Liu, J.H., Francis, A, 2004: "Theoretical analysis of local indentation on pressurized pipes," *International Journal of Pressure Vessels and Piping 81,* 931-939.